

Role of the Turbulent Magnetic Helicity in the Non-Linear Behavior of Solar Dynamo

Irina KITIAHVILI¹⁾ and Alexander KOSOVICHEV²⁾

¹⁾ *Center for Turbulence Research, Stanford University, Stanford, CA 94305, USA*

²⁾ *W.W. Hansen Experimental Physics Laboratory, Stanford University, Stanford, CA 94305, USA*

(Received: 5 September 2008 / Accepted: 29 November 2008)

Magnetic helicity plays important role in solar dynamo and magnetic field variations. It is important for explaining the observed variations of the sunspot number variations during solar cycles of activity. For comparison we consider the classical Parker's dynamo model [1] and the Kleorin-Ruzmaikin model [2]. We found that in the low-order approximation the Parker's model (without magnetic helicity) does not allow to reproduce the typical behavior of the sunspot number with a fast growth and slow decay or obtain a chaotic solution, even in strong nonlinear regimes. The analysis of the Kleorin-Ruzmaikin model shows the existence of nonlinear periodic and chaotic solutions for conditions of the solar convective zone. For this model we obtain profiles of the sunspot number variations, which qualitatively reproduce the typical profile of the solar cycles. We apply the Ensemble Kalman Filter method and show the sunspot data can be assimilated in the dynamo model. This opens perspectives for estimating the physical state of the solar dynamo and for forecasting the solar activity cycles.

Keywords: Magnetohydrodynamics, turbulence, solar dynamo, solar activity, solar magnetic fields, sunspots, data assimilation, Ensemble Kalman Filter method

1. Introduction

Solar magnetic fields are generated by a dynamo action in the turbulent plasma of the Sun's interior. One of the manifestations of solar magnetic activity is the 11-year sunspot cycle, (Fig. 1), which is characterized by the fast growth and slowly decay of the sunspot number parameter. For an explanation of the magnetic field generation Parker [1] proposed a simple dynamo model, which describes the phenomenon as an action of two factors: the differential rotation and cyclonic convective vortices. The mean-field theory and discovery of the α -effect give us a general description of the process of magnetic field generation [3].

The dynamo process is characterized by algebraic and dynamic nonlinearities. The algebraic nonlinearity can be determined as influence of the magnetic field on fluid motions and on the kinetic helicity. This results in quenching of the electromotive force and limits the growth of the magnetic field. The evolution of the small-scale magnetic helicity in the turbulent plasma causes a dynamical nonlinearity in the dynamo process. The turbulent helicity conditionally can be divided into two parts: hydrodynamic and magnetic. The kinetic helicity describes helical turbulent fluid motions; the magnetic helicity determines the order of twisted magnetic field lines. Due to the fact that the kinetic helicity makes the magnetic field small-scaled, the back influence on the turbulent fluid motions can restrict the unlimited growth of the magnetic field.

In the mean-field approach the magnetic helicity is separated into large- and small-scale components.

Because of the conservation of the total helicity a growth of the large-scale magnetic helicity due to the dynamo action is compensated by the growth of the small-scale helicity of opposite sign [4]. Thus, the small- and large-scale magnetic fields grow together and are mirror-asymmetrical and hence the condition of magnetic helicity conservation is, perhaps, more severe for a restriction of the dynamo action than the condition of the energy conservation, which leads to quenching of the kinetic helicity.

For modeling the solar cycle we consider nonlinear behavior of the Parker's dynamo model (without magnetic helicity) and the Kleorin-Ruzmaikin model, explicitly based on the idea of magnetic helicity conservation. For simplicity, we use a "low-order model" approach [5, 6], reducing the dynamo equations to a simple nonlinear dynamical system. The goal of this research is to find solutions, which can reproduce the basic properties of the sunspot number variation. To connect the dynamo model solutions with the sunspot

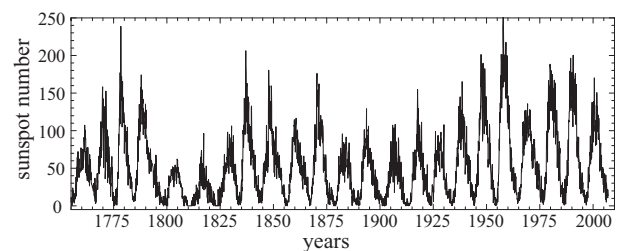


Fig. 1 Observed monthly sunspot number series for 1755 - 2007 yrs. from NGDC.

author's e-mail: irinasun@stanford.edu

number parameter we use two suggestions of Bracewell [7,8]: 1) the information about the periodical reversals of the magnetic field is included in the sunspot number series by assigning alternating positive and negative signs to the sunspot cycles, and 2) the sunspots number parameter is modeled in the form of a three-halves law: $W \sim B^{3/2}$, where W is the sunspot number, and B is the strength of the Sun's toroidal magnetic field.

2. Formulation of the Dynamo Models

It is well-known that the induction equation in the mean-field approximation [9] for the case for isotropic turbulence is written

$$\frac{\partial \langle \mathbf{B} \rangle}{\partial t} = \nabla \times (\langle \mathbf{v} \rangle \times \langle \mathbf{B} \rangle + \alpha \langle \mathbf{B} \rangle - \eta \nabla \times \langle \mathbf{B} \rangle), \quad (1)$$

where $\langle \mathbf{B} \rangle$ represents the averaged over longitude magnetic field, $\langle \mathbf{v} \rangle$ represents mean global-scale motions in the Sun (such as the differential rotation), parameter α is helicity, η describes the sum of the turbulent and molecular magnetic diffusivity $\eta = \eta_t + \eta_m$ (usually $\eta_m \ll \eta_t$).

For describing the average magnetic field, following [1], we choose a local coordinate system, xyz , where axis z will represent the radial coordinate, axis y is the azimuthal coordinate and axis x coincides with colatitude (Fig. 2). Hence, the vector of the mean field, $\langle \mathbf{B} \rangle$, can be represented as

$$\langle \mathbf{B} \rangle = B(x, y, z) \mathbf{e}_y + \nabla \times [A(x, y, z) \mathbf{e}_y], \quad (2)$$

where $B(x, y)$ is the toroidal component of magnetic field, $A(x, y)$ is the vector-potential of the poloidal field. Assuming that $\langle \mathbf{v} \rangle = v_y(x) \mathbf{e}_y$ (rotational component) we can write the dynamical system describing Parker's model of the α -dynamo [1] in the standard form:

$$\frac{\partial A}{\partial t} = \alpha B + \eta \nabla^2 A \quad (3)$$

$$\frac{\partial B}{\partial t} = G \frac{\partial A}{\partial x} + \eta \nabla^2 B, \quad (4)$$

where $G = \partial \langle v_y \rangle / \partial z$ is the rotational shear.

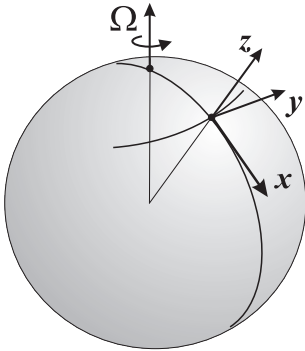


Fig. 2 Local Cartesian reference coordinate system.

Assuming that the coefficients are constants and seeking a solution of the model in the form $(A, B) \sim (A_0, B_0) \exp[i(kx - \omega t)]$, we find the well-known result [1] that a pure periodic solution exists if $D = \alpha G / \eta^2 k^3 = 2$, where D is the so-called "dynamo number". The solutions grow in time for $|D| > 2$, and decay for $|D| < 2$.

According to the periodic solution for Parker's model, profiles of variation for toroidal and poloidal components of magnetic field are sinusoidal. Therefore, model solar cycle has symmetric profile and is different from the mean profile of the solar cycle. Then, for deformation of a profile and obtaining chaotic solutions we increase the dynamo number, and following a standard procedure, we include a nonlinearity (α -quenching) as $\alpha / (1 + \xi B^2)$ [10, 11], where ξ is a quenching parameter, which limits the growth of the magnetic field amplitude. However, our numerical calculation showed that in the nonlinear regime the variations of the toroidal field and the sunspot number are also periodic and similar to the classical case of the linear harmonic solution for $|D| = 2$. Thus, in the one-mode approximation the classical Parker's dynamo model even in nonlinear cases gives only periodic oscillatory solutions, and, therefore, cannot explain the observed variations of the sunspot number in the solar cycles.

For creating chaotic variations of the magnetic field it is necessary to add to the Parker's model a third equation describing variations of the magnetic helicity and its interaction with the large-scale magnetic field [2, 12]:

$$\frac{\partial \alpha_m}{\partial t} = \frac{Q}{2\pi\rho} \left[\langle \mathbf{B} \rangle (\nabla \times \langle \mathbf{B} \rangle) - \frac{\alpha}{\eta} \langle \mathbf{B} \rangle^2 \right] - \frac{\alpha_m}{T}, \quad (5)$$

where $Q \sim 0.1$, T is characteristic time of the magnetic diffusion. Equation (5) is written for the case of an uniform turbulent diffusion, and when the magnetic Reynolds number is large, $\eta \approx \eta_t$.

For analysis of the Kleeorin-Ruzmaikin model we transform equations (3)-(5) into a nonlinear dynamical system in nondimensional variables. Following the approach of Weiss [6], we average the system of equations (3)-(5) in a vertical layer to eliminate z -dependence of A and B and consider a single Fourier mode propagating in the x -direction assuming $A = A(t)e^{ikx}$, $B = B(t)e^{ikx}$.

Note that the formulation and the interpretation of solutions of the simplified system are not straightforward because it does not adequately describes nonlinear coupling of the spatial harmonics. So, dominant modes of the toroidal field in the case of the solar dynamo are described by the harmonics [5], which are antisymmetric with respect to the equator (in accordance with the Hale law), $\sin(kx)$, where x is colatitude, and the wavenumber, k , is even: $k = 2, 4, \dots$

The first $k = 2$ harmonic has the largest growth rate. We retain only this mode in our dynamical model. Then equations (3)-(5) in nondimensional variables became [13]

$$\begin{aligned}\frac{dA}{dt} &= DB - A, \\ \frac{dB}{dt} &= iA - B, \\ \frac{d\alpha_m}{dt} &= -\nu\alpha_m + [AB - D(B^2 - \lambda A^2)],\end{aligned}\quad (6)$$

where $D = D_0\alpha$ and $\alpha = \alpha_h + \alpha_m$ are the nondimensional dynamo number and total helicity that is the sum of kinetic and magnetic helicities, $D_0 = \alpha_0 Gr^3/\eta^2$, $\alpha_0 = 2Qkv_A^2/G$, r is a layer radius, v_A is the Alfvén speed, $\nu = T_0/T$, T_0 is characteristic time of the turbulent diffusion [2] and $\lambda = (k^2\eta/G)^2 = \text{Rm}^{-2}$, k is a characteristic wavelength, Rm is the magnetic Reynolds number.

3. Periodic and chaotic solutions

In order to estimate the range of parameters of the Kleerorin-Ruzmaikin model (3)-(5), and for modeling the solar cycle we used the standard model of the interior structure of the Sun for the top, bottom and middle areas of the convective zone. The key parameter of the model is the dynamo number $D = D_0\alpha_h$, because its magnitude determines behavior of the magnetic field, which depends on the rotational velocity and magnetic field strength. Parameter λ determines the influence of vector-potential A on variations of magnetic helicity α_m . From our estimates it follows that for the solar conditions $\lambda \leq 10^{-4}$. Consequently, we can neglect the term with λ . The nondimensional parameter, ν , describes the ratio of two characteristic times of turbulent (T_0) and magnetic (T) diffusivities. In the absence of helicity fluxes the value of the damping parameter ν is small. However, in reality the helicity fluxes increase the dissipation rate. This can be modeled as a damping term, which increases the effective value of ν [14]. Because of this the value of ν is to some extent uncertain.

Thus, for the Kleerorin-Ruzmaikin model, given by equations (3)-(5), the linear instability condition is also $|D| \equiv |\alpha_h D_0| > 2$. However, in this case the profile of the periodic solutions is not sinusoidal, and depends on the initial conditions, A_0 and B_0 . For higher initial values the amplitude of the nonlinear oscillations in the stationary state is higher. However, the shapes of the oscillation profiles are similar.

Figure 3 illustrates solutions for the model of Kleerorin-Ruzmaikin, and the corresponding variations of the sunspot number for different initial conditions. As mentioned, changes of initial values for magnetic field components A_0 and B_0 leads to very similar profiles. In high amplitude cases, dual peaks may ap-

pear in the variations of the vector potential, A , of the poloidal field. The evolution of the magnetic helicity represents a relatively smooth growth followed by a sharp decay. The helicity has maxima when the toroidal field is zero. In these calculations the value of parameter ν , which describes damping rate of magnetic helicity and depends on the turbulence spectrum and the dissipation through helicity fluxes, is of the order of unity. Finally, the variations of the sunspot number, W , with the amplitude increase are characterized by higher peaks and shorter rising times (Fig. 3d). Note that in the sunspot number profile we can recognize the well-known general properties of the sunspot number profile with the rapid growth at the beginning of a cycle and a slow decrease after the maximum.

With the increase of $|\alpha_h D_0|$ ($|\alpha_h D_0| > 2$) the profile of magnetic field variations continue to deform and can become unstable with very steep variations of the magnetic field. The solution can be stable again if we enhance the back reaction by increasing the quenching parameter. We use the following quenching formula for the kinetic part of helicity, α_h , [12] $\alpha = \alpha_h/(1 + \xi B^2) + \alpha_m$. Thus we always have a possibility for selecting ξ to obtain periodic nonlinear solutions.

The transition of the periodic to chaotic solutions occurs when the dynamo number, $|\alpha_h D_0|$, increases. In the transition regime the cycle amplitude becomes modulated: it slowly increases with time, and then suddenly and very sharply declines, and then start growing again [13].

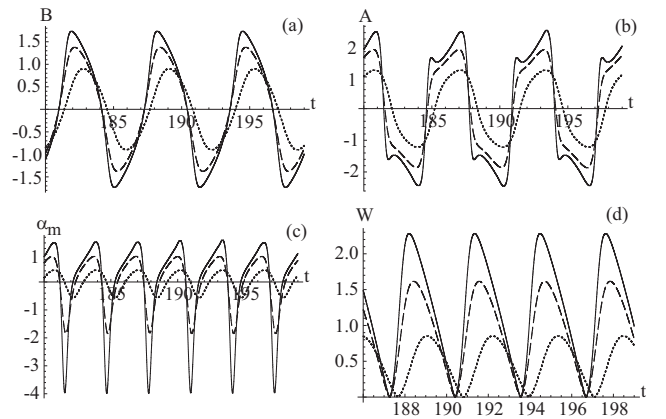


Fig. 3 Variations of the magnetic field for the middle convective zone $\alpha_h D_0 = -2$: $\nu = 1.28$, $\alpha_h = 2.439$, $D_0 = -0.82$ for different initial conditions: $B_0 = 4i$, $A_0 = -0.01i$ (dotted curve), $B_0 = 4i$, $A_0 = -i$ (dashed curve) and $B_0 = 1 + 4i$, $A_0 = -i$ (black curve): a) toroidal component, B ; b) vector-potential, A , of the poloidal magnetic field; c) magnetic helicity variations; d) evolution of the model sunspot number.

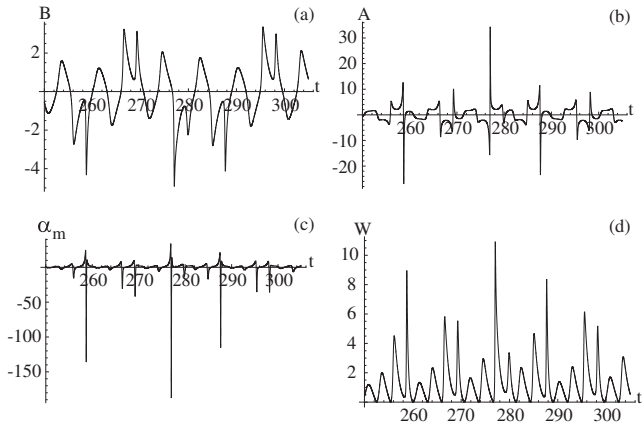


Fig. 4 Example of the chaotic solution for: a) toroidal field B , b) vector-potential A , c) magnetic helicity α_m , d) model sunspot number W and e) the phase portrait of the magnetic components.

In the case of significant deviations from the condition of linear stability the solutions become chaotic for all variables of the dynamical system. Figure 4 shows an example of chaotic variations for the middle convective zone parameters: $\nu = 1.28$, $\lambda = 1.23 \times 10^{-6}$, $D_0 = -0.82$, $\alpha_h = 3.2$, $\xi = 3.9 \times 10^{-3}$ for the magnetic field components, the magnetic helicity and the sunspot number parameter [13]. In the chaotic solutions, the peaks of the toroidal magnetic field, B (Fig. 4a) strongly correlate with the peaks of the vector-potential, A , and the magnetic helicity, α_m , (Fig. 4b, c). The growth of the toroidal field also leads to strengthening of the poloidal field and strong fluctuations of the magnetic helicity.

Now we can see from Figs. 3d and 4d that the profiles of the model sunspot number variations qualitatively describe the mean profile of the solar cycles. The next important characteristic of the solar cycles is the relationship between the amplitude and the growth time. Fig. 5 shows this relationship for some periodical solutions (panel a), four chaotic solutions (panel b) and properties for the real 23 solar cycles (panel c). In the case of the relationship for the periodic solutions (panel a) the circles show a sequence for a fixed value of the kinetic helicity, $\alpha_h = 2.44$ and the dynamo number varying from -7 to -0.82 , the crosses show the case of fixed $D_0 = -0.82$ and varying α_h , from 2.44 to 3 . The size of the crosses and circles is proportional to the corresponding values of $|D_0|$ and α_h . The four chaotic solutions shown in panel b) are obtained for $D_0 = -0.82$ and different values of the kinetic helicity: $\alpha_h = 2.8$ (black circles), $\alpha_h = 3$ (empty circles) and $\alpha_h = 3.2$ (stars). The time scales are non dimensional. The bottom panel (Fig. 5c) shows the observed amplitude-growth time properties of the solar cycles of 1755 - 2007. Thus, all three panels demonstrate that the growth time is

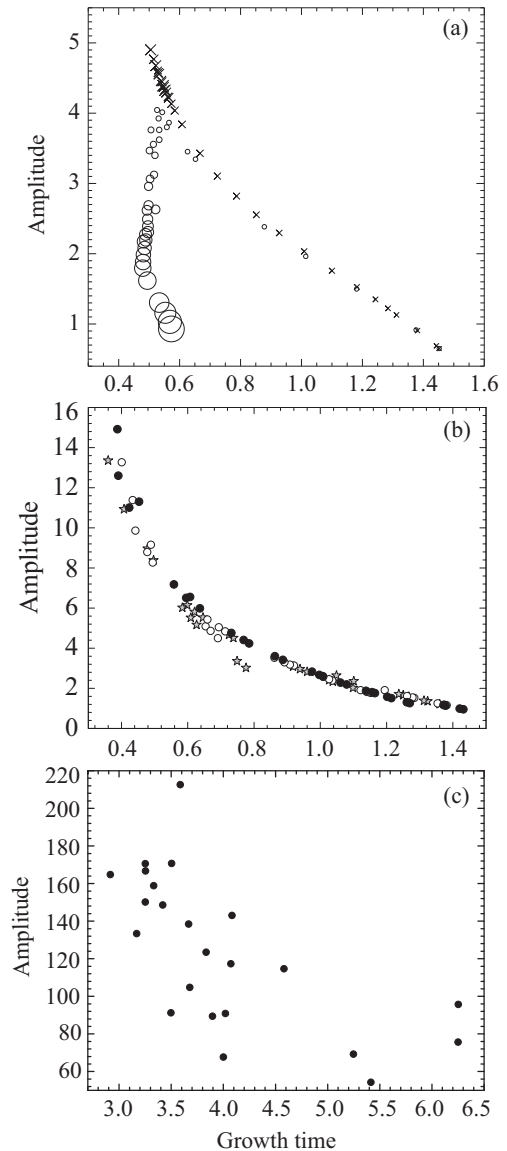


Fig. 5 Relationships between the amplitude of the model sunspot number and the growth time for a) periodic solutions; b) chaotic solutions (for $D_0 = -0.82$ and different values of the kinetic helicity); and c) for real solar cycles.

shorter for stronger cycles.

4. Assimilation of Sunspot Data into the Dynamo Model

Despite the fact that the Kleorin-Ruzmaikin dynamo model reproduces the basic properties of a solar cycle, it has significant deviations from the actual sunspot data. This problem is related to inaccuracies of the model, which contains various assumptions and approximations, unknown initial conditions, and errors of the observational data. Data assimilation methods allow us to use the observed information and obtain the best estimate of the model physical state.

In the case of non-linear systems the Ensemble

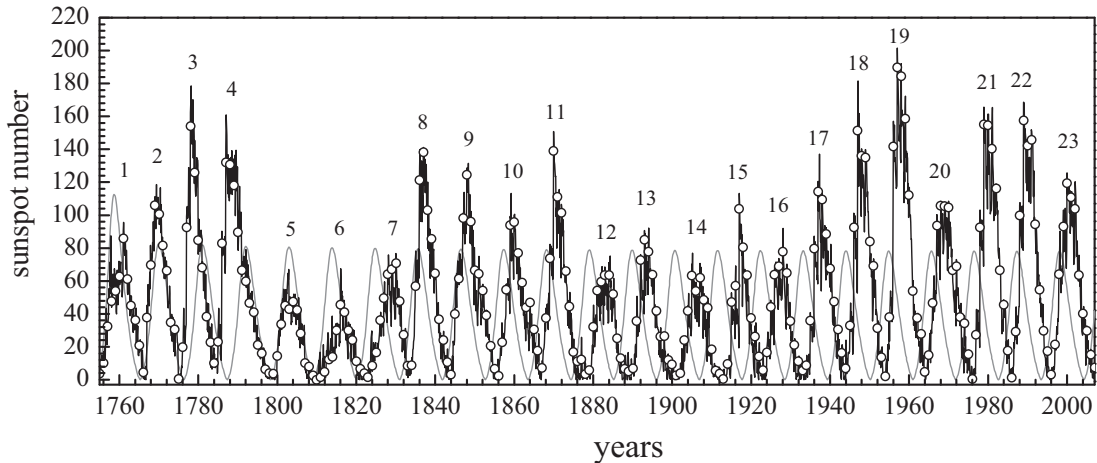


Fig. 6 Results of assimilation for the known observational data of the annual sunspot number (circles). The grey curve shown the reference solution (without assimilation analysis), and the black curve shows the EnKF estimate of the sunspot number variations, obtained from the data and Kleeorin-Ruzmaikin dynamo model. Numbers from 1 to 23 are the conventional numbering of the sunspot cycles.

Kalman Filter (EnKF) is shown to be an effective method for data assimilation [15]. This method is based on the standard Kalman Filter and includes a statistical analysis of ensembles of possible solutions. The main difference of the EnKF from the standard Kalman Filter is in using for the analysis an ensemble of possible states of a system, which can be generated by the Monte Carlo simulations.

Figure 6 shows the result of assimilation of the annual sunspot number data (circles) into Kleeorin-Ruzmaikin model by the EnKF method. For comparison the figure shows an exact solution of the model (grey curve) without assimilation and the best estimate of the sunspot number variations (black curve) obtained by the EnKF method from the dynamo model calculations. It reproduces well the observational data (Fig. 1). The errors are estimated by modeling the model uncertainties by a random forcing function and assuming a 14% error in the data. This result provides a basis for developing physics-based methods of predicting the solar activity cycles.

5. Conclusion

In the mean-field theory the dynamo process is described in terms of plasma helicity, which has two components: kinetic, caused by helical motions, and magnetic. The dynamo theories often include only the kinetic part. However, it has been suggested that the magnetic helicity may also play a significant role. Using a low-order dynamical system approach we examine the influence of the kinetic and magnetic helicities on the non-linear fluctuations of the dynamo-generated magnetic field in the conditions of the solar plasma, and compare these with the sunspot number variations observed during the solar 11-year cycles.

For comparison, we consider the classical Parker's dynamo model [1] and the Kleeorin-Ruzmaikin model [2]. We find that the Parker's model (which does not take into account the magnetic helicity) does not allow reproducing the typical behavior of the sunspot number with a fast growth and slow decay or obtaining a chaotic solution, even in strong nonlinear regimes.

The analysis of the Kleeorin-Ruzmaikin model, which describes the evolution of the magnetic helicity based on the balance between the large-scale and turbulent magnetic helicities, shows the existence of nonlinear periodic and chaotic solutions for conditions of the solar convective zone. For this model we obtained the profiles of the sunspot number variations, which qualitatively reproduce the typical profile of the solar cycles. Also, the Kleeorin-Ruzmaikin model has been used for assimilating the sunspot data by applying the Ensemble Kalman Filter method. The initial results show that this assimilation method works for this model reasonably well, and can be used for predicting solar sunspot cycles.

This work was supported by the Center for Turbulence Research (Stanford) and the International Space Science Institute (Bern).

- [1] E.N. Parker, *Astrophys. J.* **122**, 293 (1955).
- [2] N.I. Kleeorin and A.A. Ruzmaikin, *Magnetohydrodynamics* **18**, 116 (1982).
- [3] F. Krause and K.-H. Rädler, *Mean-field magnetohydrodynamics and dynamo theory* (Pergamon Press, Oxford, 1980) p. 332.
- [4] D. Sokoloff, *Plasma Phys. Control. Fusion*, **49**, B447 (2007).
- [5] D.D. Sokoloff and S.N. Nefyodov, *Vychislitelnyye metody i programmirovaniye* **8**, 195 (2007), (in Russian, www.srcc.msu.ru).
- [6] N.O. Weiss *et al.*, *Geophys. Astrophys. Fluid Dynamics*, **30**, 305 (1984).

- [7] R.N. Bracewell, *Nature*, **171**, 649 (1953).
- [8] R.N. Bracewell, *Mon. Not. R. Astr. Soc.*, **230**, 535 (1988).
- [9] H.K. Moffatt, *Magnetic field generation in electrically conducting fluids* (Cambridge Univ. Press, New York, 1978) p. 343.
- [10] A. Brandenburg and K. Subramanian, *Physics Reports*, **417**, 1 (2005).
- [11] T.S. Ivanova and A.A. Ruzmaikin, *Sov. Astron.*, **21**, 479 (1977).
- [12] N. Kleeorin *et al.*, *Astron. Astrophys.*, **297**, 159 (1995).
- [13] I.N. Kitiashvili and A.G. Kosovichev, *Geophys. Astrophys. Fluid Dynamics*, (2008) in press.
- [14] E.G. Blackman and A. Brandenburg, *Astrophys. J.*, **584**, L99 (2003).
- [15] G. Evensen, *J. Geophys. Res.*, **99**(C5), 10143 (1994).